The ground turbulent boundary layer of a stationary tornado-like vortex[1]

By S. W. CHI, S. J. YING and C. C. CHANG, *Department of Space Science and Applied Physics, The Catholic University of America, Washington, D.C.*

(Manuscript received September 9, 1968; revised version March 10, 1969)

ABSTRACT

Recently, experimental data became available on the ground turbulent boundary layer of a model tornado vortex. A comparison with early theories of Weber, Anderson, Rott and Lewellen is made and it is found that the root-mean-square error seems great and justifies development of an improved theory with newly specified velocity profiles which are close to the experimental data. The dependence of the boundary layer development on the Reynolds number is explicitly shown. The present theory also extends to the useful Reynolds number range of the natural tornado.

1. Introduction

The ground boundary layer of a tornado is highly turbulent due to the ground surface roughness and the large size of the storm. The visual core of the tornado is not stationary but travels and rotates at high speed. It is difficult, if not impossible, to carry out instrument measurements. At the Catholic University of America, a first crucial step of simplified simulation was to devise a stationary laboratory model of the turbulent tornado-like vortex touching a circular disk, as shown in Fig. 1. A volume of measured data on the turbulent boundary layer of tornado-like vortices was obtained by Ying & Chang (1968). It was found that the rotational flow outside the ground boundary layer and the vortex core behave like a potential vortex. The present paper is intended to compare the above boundary-layer data with available theories and to develop a new theory with the guidance of the available experimental data.

In the theoretical study of the turbulent boundary layer, the three works of Weber (1956), Anderson (1961) and Rott & Lewellen (1964) are all based on the momentum-integral method originally developed by von Karman (1921) who considered the flow problem of a finite rotating disc. Each of the above three works used the similarity hypothesis and specified some reasonable velocity profiles and ground shear-stress laws. However, it was found that their specified velocity profiles deviate appreciably from the measured velocities of Ying & Chang (1968). Fairly high root-mean-square errors were computed as will be shown later. Some improvement in the treatment was needed. This led the present authors to specify some new velocity profiles and shear-stress laws which fitted the measured data more closely. Also by nature of the present treatment which is described in Section 3 below, the work extends to the Reynolds number range of the natural tornado.

2. Survey of previous theoretical works

Table 1 summarizes the main features of their contributions and the explanation of its significance will be given in Section 2.2. It will be noted that the theories have much in common with one another. One reason for the similarity is they have been based upon the momentum-integral method developed by von Karman (1921) for the problem of the turbulent boundary layer on a finite rotating disc, which was also applied by Taylor (1950) to the problem of the present type for the laminar boundary layer.

[1] This work is supported by the National Science Foundation under Grant GP 757.

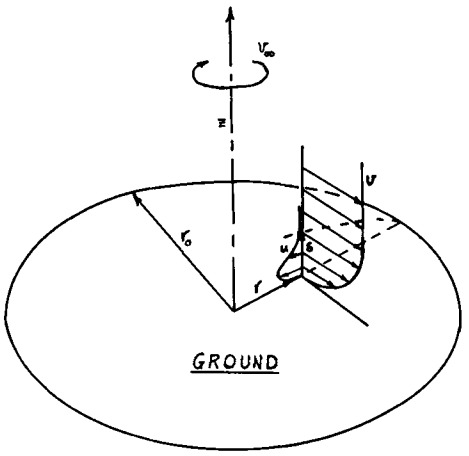

Fig. 1. Sketch of the ground boundary layer of a model tornado vortex.

2.1 *General formulation*

The theories mentioned in Table 1 are all based upon the same basic assumptions which were used by von Karman & Taylor for their problems mentioned above. These are: (i) the flow is steady and axisymmetrical; (ii) the fluid properties are uniform; (iii) the boundary layer has a finite thickness; (iv) the pressure does not change across the boundary-layer thickness; (v) the radial velocity outside the boundary layer is negligibly small in comparison with the tangential velocity at the same position; (vi) both the radial and the tangential components of the velocity are respectively similar in profiles and, (vii) von Karman's adaption of the two-dimensional shear-stress law for the turbulent boundary layer to the three-dimensional case is accepted.

When the first five assumptions are used, it was shown by earlier investigators of Table 1 that the boundary layer tangential and radial momentum-integral equations are as follows:

$$\frac{d}{dr}\left(r^2\int_0^\delta uvdz\right) - rv_\infty\frac{d}{dr}\left(r\int_0^\delta udz\right) = -\frac{\tau_t r^2}{\varrho}, \tag{1}$$

$$\frac{d}{dr}\left(r\int_0^\delta u^2dz\right) + \int_0^\delta (v_\infty^2 - v^2)dz = -\frac{\tau_r r}{\varrho}, \tag{2}$$

where τ_t and τ_r are the tangential and radial components of the ground shear stress, ϱ is the density, and the meanings of other symbols are shown in Fig. 1.

On the use of the remaining assumptions, i.e. (vi) and (vii), the velocity components following Taylor (1950) and the ground shear-stress components following Karman (1921) are written in these forms:

$$u(\xi,\eta) = v_\infty(\xi)E(\xi)f(\eta), \tag{3}$$

$$v(\xi,\eta) = v_\infty(\xi)g(\eta), \tag{4}$$

$$\tau_{res}(\xi) = c\varrho v_\infty^2(1+E^2)\left(\frac{\nu}{v_\infty\delta\sqrt{1+E^2}}\right)^\beta, \tag{5}$$

$$\tau_r(\xi) = c\varrho v_\infty^2 E\sqrt{1+E^2}\left(\frac{\nu}{v_\infty\delta\sqrt{1+E^2}}\right)^\beta, \tag{6}$$

$$\tau_t(\xi) = c\varrho v_\infty^2\sqrt{1+E^2}\left(\frac{\nu}{v_\infty\delta\sqrt{1+E^2}}\right)^\beta. \tag{7}$$

In these equations ξ is the non-dimensional radius defined as r/r_0, η the non-diemnsional distance from the ground defined as z/δ, E the unknown radial velocity amplitude, $f(\eta)$ the specified similar radial velocity function, $g(\eta)$ the specified similar tangential velocity func-

Table 1. *Comparison of theories*

Authors	C	β	$g(\eta)$	$f(\eta)$	*rms* error	Remarks
Weber (1956)	0.0225	0.25	$\eta^{1/7}$	$\eta^{1/7}-\eta$	9.8	Discussed in Section 2
Anderson (1961)	0.0225	0.25	$\eta^{1/7}$	$\eta^{1/7}-13/7\,\eta+6/7\,\eta^2$	12.5	Discussed in Section 2
Rott & Lewellen (1964)	0.0225	0.25	$\eta^{1/7}$	$\eta^{1/7}(1-\eta^2)$	13.6	Discussed in Section 2
Present theory	Variable	Variable	$\eta^{1/\alpha}$	$\frac{1}{2}\eta^{1/\alpha}(1+\cos\pi\eta)$	5.4	Variable c, α, β Values see Table 2 Discussed in Sec. 3

tion, τ_{res} the resultant ground shear stress, ν the molecular kinematic viscosity, c a constant of the shear-stress law and β an exponential of the shear-stress law.

On the substitution of (3) through (7) into (1) and (2), the two resultant equations for the potential vortex outer flow, i.e. $\bar{v}_\infty \equiv v_\infty/v_0 = 1/\xi$,[1] after somewhat lengthy but straightforward calculations, can be written as:

$$\frac{dE^2}{d\xi} = \left(\frac{2}{\xi}\right)E^2 - \left[2c\left(\frac{1}{I_2} + \frac{1}{I_1 - I_4}\right)\xi^\beta\right] \times \frac{E^2(1+E^2)^{(1-\beta)/2}}{E\delta_1^{1+\beta}} - \left(2\frac{I_3}{I_2}\frac{1}{\xi}\right), \quad (8)$$

$$\frac{dE\delta_1^{1+\beta}}{d\xi} = -\left(\beta\frac{1}{\xi}\right)E\delta_1^{1+\beta} + \left(\beta\frac{I_3}{I_2}\frac{1}{\xi}\right)\frac{E\delta_1^{1+\beta}}{E^2} + \left[c\left(\frac{\beta}{I_2} - \frac{1+2\beta}{I_1 - I_4}\right)\xi^\beta\right](1+E^2)^{(1-\beta)/2}, \quad (9)$$

where δ_1 is the unknown non-dimensional boundary layer thickness defined as $(\delta/r_0)(v_0 r_0/\nu)^{\beta/(1+\beta)}$ and the integrals I_1, I_2, I_3 and I_4 are defined by the equations:

$$I_1 \equiv \int_0^1 f d\eta; \qquad I_2 \equiv \int_0^1 f^2 d\eta;$$
$$I_3 \equiv \int_0^1 (1-g^2)d\eta; \quad I_4 \equiv \int_0^1 fg d\eta. \quad (10)$$

Equations (8) and (9) are derived on the assumptions used by all authors of Table 1. They are written here in a form suitable for numerical integration and convenient for comparison among the various theories. When the constant c and exponent β for the shear-stress law and the velocity functions $f(\eta)$ and $g(\eta)$ are specified, these equations can be used to evaluate the non-dimensional boundary-layer thickness $\delta_1(\xi)$ and the radial velocity amplitude $E(\xi)$ in a straightforward manner. For example, to start these equations (8) and (9) from $\xi = 1$ where E^2 and $E\delta_1^{1+\beta}$ are zero, we shall expand E and $E\delta_1^{1+\beta}$ in a power series of $(1-\xi)$ and assume that for a small change in ξ the first term of the series is valid. Hence, we can start (8) and (9) by taking $d\xi = \delta\xi = -0.005$ and expressing the variables E^2 and $E\delta_1^{1+\beta}$ as:

$$E^2 = c_1(1-\xi); \quad E\delta_1^{1+\beta} = c_2(1-\xi) \quad (11)$$

Substituting (11) into (8) and (9) we can solve for c_1 and c_2 and obtain in this way the values of E^2 and $E\delta_1^{1+\beta}$ at $\xi = 0.995$. From then on Euler's finite-difference forms of (8) and (9) are employed and the solution obtained stepwise to $\xi = 0.05$.

2.2 *Comparison among previous theories*

From the above formulation, it is seen that the theoretical predictions of the boundary-layer behavior are dependent mainly on the specification of the functions $f(\eta)$ and $g(\eta)$ and the choice of the values of c and β. Table 1 shows the c- and β-values and $f(\eta)$- and $g(\eta)$-functions used by the various authors.

2.3 *Comparison of the previous theories with experiments*

As mentioned above, some data on turbulent boundary layer of a tornado-like vortex has been obtained by Ying & Chang in experiments on a model tornado, the details of which and the instrumentation are described elsewhere by Ying & Chang (1968). Briefly, a concentrated vortex is produced by a rotating screen cylinder of 1.98 m in diameter and an exhaust fan mounted on the top of the cylinder. The velocity components in the ground boundary layer are measured by hot film anemometers. Measurements have been made at three different conditions, namely: (i) Re_t ($\equiv v_0 r_0/\nu$ or Γ/ν) $= 2.2 \times 10^4$; (ii) $Re_t = 4.3 \times 10^4$; (iii) $Re_t = 6.1 \times 10^4$. Under all three conditions v_∞ is found to be inversely proportional to r except for the region close to the vortex core. As an example, v_∞, and u and v distributions of the boundary layer for the condition of $Re_t = 4.3 \times 10^4$ are shown in Figs. 2. 3 and 4, respectively.

To test the accuracy of the various theories, the theoretical boundary-layer velocity profiles will be compared with all experimental data under the three conditions mentioned above. Although approximations are sometimes used in the evaluation of the momentum-integral equations, for example see Rott & Lewellen (1964), the error introduced by these approximations is uncertain. We shall numerically evaluate (8) and (9).

With the use of the c, β, $f(\eta)$ and $g(\eta)$ for the

[1] In fact, $\bar{v}_\infty$ goes to zero instead of infinity as $\xi \to 0$ and does not follow the potential vortex in the vortex core where the theory is not valid.

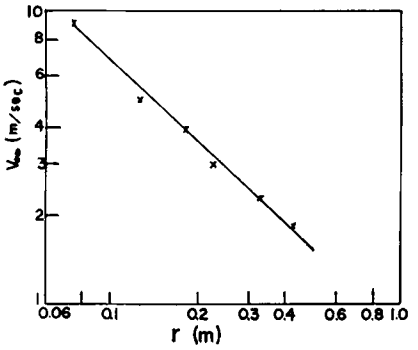

Fig. 2. Tangential velocity for the outer flow measured at $\mathrm{Re}_t = 4.3 \times 10^4$

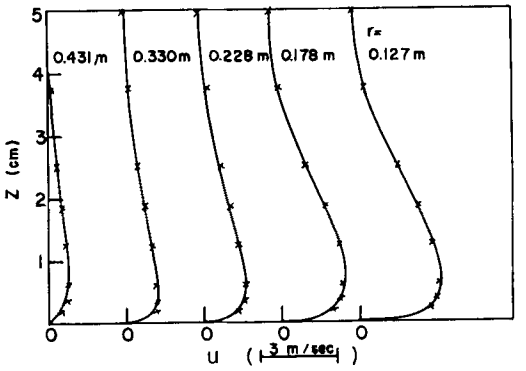

Fig. 3. Radial velocity in the boundary layer measured at $\mathrm{Re}_t = 4.3 \times 10^4$.

different theories of Table 1, the theoretical values of $E(\xi)$ and $\delta_1(\xi)$ are obtained by integration of (8) and (9) as described in section 2.2. Consequently, the theoretical boundary-layer velocities at various r and z are evaluated for each theory by (3) and (4) with the $f(\eta)$ and $g(\eta)$ functions shown in Table 1.

The accuracy of the various theories can only be judged by comparison of the experimental data with the theoretical data for the conditions of the experiments. The criterion used is the smallness of the *rms* values of the difference between the theoretical and the experimental velocity functions, i.e. the difference between f_{th} and f_{exp} ($\equiv u_{\mathrm{exp}}/v_\infty E_{\mathrm{th}}$) or the difference between g_{th} and g_{exp} ($\equiv v_{\mathrm{exp}}/v_\infty$). The evaluated *rms* values for the different theories, shown in Table 1, range from 9.8 percent to 13.6 percent for the various theories.

3. Development of an improved theory

3.1 *Formulation*

The present theory adapts essentially the same assumptions and formulation as the other theories, i.e. (8) and (9) used by other authors are also used here. Different boundary-layer velocity and ground shear-stress functions are introduced for the present theory (Table 1). The reason for these choices will be explained below.

3.2 *Ground shear-stress law*

The shear-stress laws for the various theories are defined by (5) through (7) and Table 1. These laws for all the previous theories reduce for the two-dimensional case (i.e. for $E = 0$) to the Blasius shear-stress law. That is,

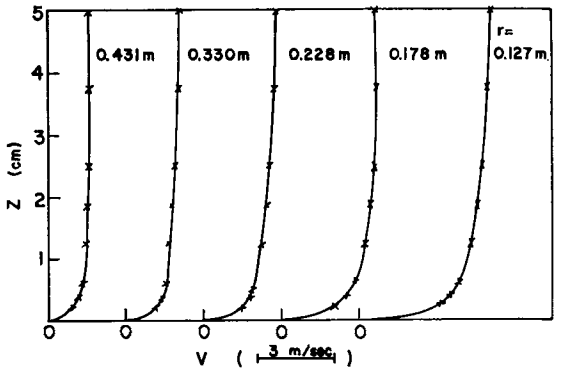

Fig. 4 Tangential velocity in the boundary layer measure at $\mathrm{Re}_t = 4.3 \times 10^4$.

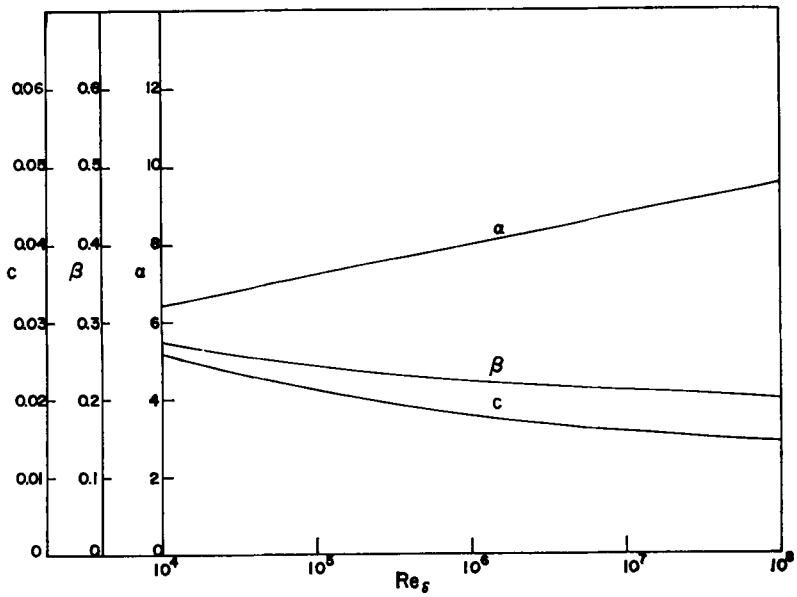

Fig. 5. c-, α-, and β-values versus Reynolds number based upon boundary-layer thickness.

$$\tau = 0.0225\,\varrho v_\infty^2 \left(\frac{\nu}{v_\infty \delta}\right)^{0.25} \qquad (12)$$

However, a better shear-stress law (e.g. Schlichting 1968, pp. 564–566) for the two-dimensional case is:

$$\tau = c\varrho v_\infty^2 \left(\frac{\nu}{v_\infty \delta}\right)^{\beta} \qquad (13)$$

where c and β are no longer constants but functions of Re ($\equiv v_\infty\, \delta/\nu$) as shown by Fig. 5.

Comparison of the shear-stress law of (13) and the Blasius shear-stress law of (12) with the two-dimensional experiments of Schultz-Grunow (1941), Hama (1941), Wieghart (1944) and Ludwig & Tillman (1949) is shown by Fig. 6. (13) is seen to give better agreement with the experiments than does the Blasius law (12).

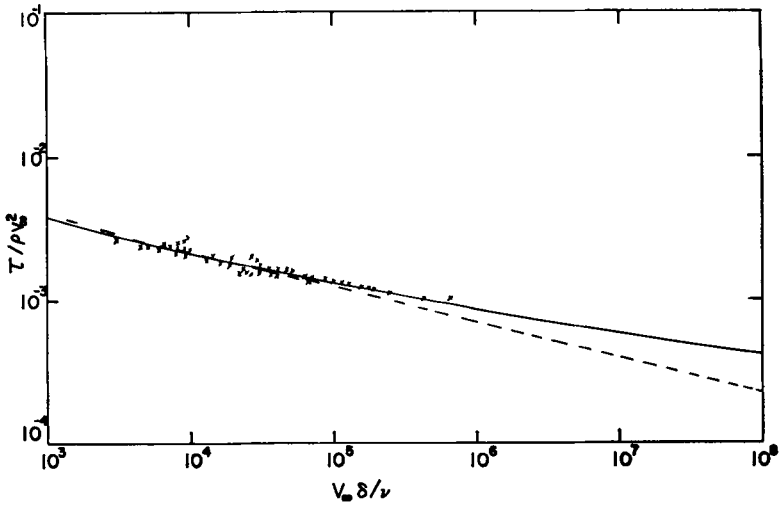

Fig. 6. Nondimensional wall shear stress versus Reynolds number based upon boundary-layer thickness. ---, theory equation (12); —, theory equation (13); ×, experiments.

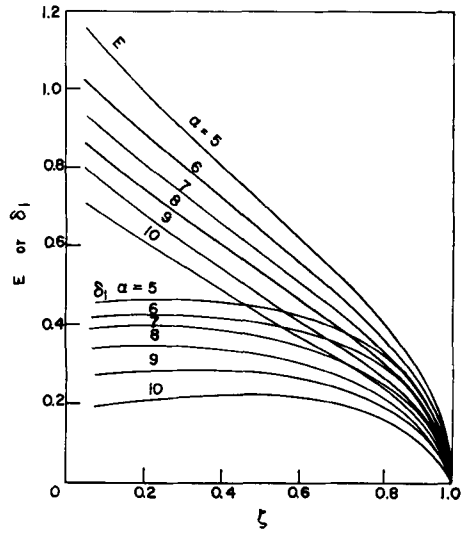

Fig. 7. Nondimensional boundary-layer thickness and radial-velocity amplitude predicted by the present theory.

Following the above comparison, we shall adapt the two-dimensional shear-stress law of (13) instead of (12) for the present problem. Hence, we have used the shear-stress law of (5) through (7) with c- and β-values being variables.

3.3 *Boundary-layer velocity functions*

The velocity laws for the present theory, as for the previous theories, are written in the forms of (3) and (4). The $f(\eta)$ and $g(\eta)$ functions of (3) and (4) (Table 1) for the previous theories have the general forms of $f(\eta) = \eta^{1/7}(1-\eta)^m$ or $\eta^{1/7} + a\eta + b\eta^2$ and $g(g) = \eta^{1/7}$. In these expressions, the term $\eta^{1/7}$ is related to β being equal to 1/4 (Lin 1959, pp. 121–123).

As our shear-stress is given by (5) through (7) with β being variables, the term corresponding to $\eta^{1/7}$ for the other theories now become $\eta^{1/\alpha}$. The values of α are related to β by the equation $\alpha = (2-\beta)/\beta$ (Lin 1959, pp. 121–123). Hence, we have used as a $g(\eta)$ function for the present theory:

$$g(\eta) = \eta^{1/\alpha}, \tag{14}$$

where α as a variable and related to β by the equation $\alpha = (2-\beta)/\beta$.

With the $g(\eta)$ functions determined above, the $f(\eta)$ function can be written, following the other authors, as $f(\eta) = \eta^{1/\alpha}(1-\eta)^m$ or $\eta^{1/\alpha} + a\eta + b\eta^2$. However, it was found that better agreement between the theory and the experiments was obtained by choosing

$$f(\eta) = 1/2\eta^{1/\alpha}(1+\cos \pi\eta),$$

which satisfies the boundary consitions $f(0) = f(1) = f'(1) = 0$.

3.4 *Variation of c, α and β values*

The direct adaption of the two-dimensional shear-stress law of (13) for the present problem requires c-, α- and β-values as function of Re_δ,[1] it makes the integration of the momentum equations complicated. To facilitate numerical calculations, it is desirable to use mean values of c, α and β for a vortex of known circulation strength. For this purpose the mean values of c, α and β versus $\mathrm{Re}_t (\equiv \Gamma/\nu)$ are to be derived.

With the use of the different mean values of c, α and β, momentum-integral (8) and (9) have been evaluated. The resultant non-dimensional boundary-layer thickness δ, and the radial velocity amplitude E are plotted versus the non-dimensional ξ in Fig. 7. In this figure only the mean values of α are indicated; the corresponding mean values c, β and Re_δ are implied by α, shown in Fig. 5.

Below, we shall assume that the mean values of c, α, β and Re_δ can be referred to their respective values at an appropriate reference radius; and derive the mean values of c, α, β and Re_δ as functions of Re_t. By definitions of the various quantities, it can be shown that for a potential vortex:

$$\mathrm{Re}_t = \left[\frac{\xi}{\delta_1(\xi)\sqrt{1+E^2(\xi)}}\mathrm{Re}_\delta\right]^{(3+\alpha)/(1+\alpha)}. \tag{16}$$

By evaluating the quantities of the above equation at a reference radius, ξ_R, (16) becomes:

$$\mathrm{Re}_t = \left[\frac{\xi_R}{\delta_1(\xi_R)\sqrt{1+E^2(\xi_R)}}\mathrm{Re}_\delta\right]^{(3+\alpha)/(1+\alpha)} \tag{17}$$

The relation between α and Re_δ in (17) can be read from Fig. 5, and the relation between Re_t and α can be obtained with the aid of Fig. 7, if ξ_R is specified. Satisfactory results have been obtained with ξ_R equal to 1/2. Table 2 shows the derived mean values of c, α, β versus Re_t.

[1] Re_δ for the present problem is defined as $v_\infty \delta\sqrt{1+E^2}/\nu$, which is implied by equations (5) through (7).

Table 2. *c-, α-, and β-values versus* Re_t *for the present theory.*

Re_t	9×10^3	4×10^4	1.6×10^5	1.96×10^6	3.8×10^7	8.9×10^{10}
c	0.038	0.0286	0.0225	0.0178	0.0145	0.0122
α	5	6	7	8	9	10
β	0.33	0.286	0.25	0.222	0.200	0.182

3.5 *Summary of the present theory*

For a potential vortex of known Re_t values of c, α and β can be obtained (Table 2). The values of c, α and β are used to evaluate the coefficients of (8) and (9) (Table 1). (8) and (9) are then integrated numerically to obtain $E(\xi)$ and $\delta_1(\xi)$.

Alternatively, as (8) and (9) for different values of α, etc., have already been evaluated and the results plotted in Fig. 7; $E(\xi)$ and $\delta_1(\xi)$ values for Re_t in question can be read from the appropriate curve of Fig. 7.

3.6 *Comparison with experiments*

For the quantitative comparison of the present theory with the experiments and the other theories, the root-mean-square error for the present theory has also been evaluated. The present theory gives a *rms* error of 5.4 percent; while the other theories have a *rms* error ranging from 9.8 percent to 13.6 percent (Table 1).

Also for visual comparison, theoretical $f(\eta)$ and $g(\eta)$ functions for Re_t ranging from 9×10^3 to 1.6×10^5 and the experimental $f(\eta)$ and $g(\eta)$ functions for Re_t ranging from 2.2×10^4 to 6.1×10^4 are plotted in Figs. 8 and 9. These figures also show good agreement between the present theory and the experiments.

4. Conclusion

In conclusion, the results of this work are summarized below:

(i) This is the first time a theory has been developed for a turbulent boundary layer of a tornado-like vortex with the guidance of available experimental data.

(ii) In comparison with the previous theory, the optimum choices of the velocity profiles of u and v are judged from the *rms* errors with the experimental data, which presently gives the lowest *rms* error.

(iii) The dependence of the ground shear-

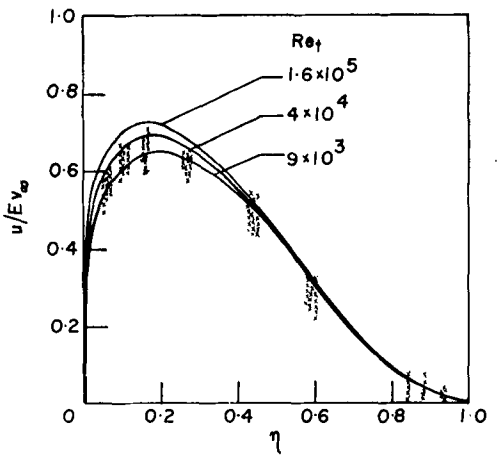

Fig. 8. Comparison of theoretical and experimental radial velocity function. —, Present theory Re_t from 9×10^3 to 1.6×10^5; ×, experiments Re_t from 2.2×10^4 to 6.1×10^4.

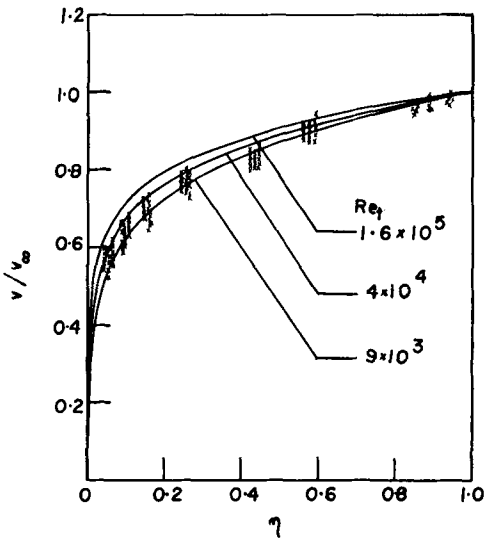

Fig. 9. Comparison of theoretical and experimental tangential velocity function. —, Present theory Re_t from 9×10^3 to 1.6×10^5; experiments Re_t from 2.2×10^4 to 6.1×10^4.

stress and boundary layer velocity profiles on the Reynolds number is taken into account for the first time. Although experimental data of the ground shear-stress for the tornado-like vortex outer flow are not presently available, the dependence of wall shear-stress for two-dimensional flow on the Reynolds number is well known, tentatively chosen, and is clearly shown by Fig. 6. By comparison of the *rms* values shown in Table 1 for this theory with that of the other theory, the improvement made by taking the Reynolds number into account can be seen.

(iv) The dependence of δ, and E on Reynolds number predicted by the present theory is shown in Fig. 7. With the available limited range of experimental data on the tornado model, the present theory can be used to predict the boundary layer velocity profiles and thickness to a large range of Reynolds number.

We have now some preliminary understanding about the structure of the tornado boundary layer. At present, however, knowledge for the region of the vortex-core root is very limited. Further work, both theoretical and experimental, is needed.

Acknowledgments

This work was supported by the National Science Foundation under Grant GP 757. The authors would like to express their gratitude to Drs. Paul Rispin and D. P. Wang for their helpful comments on an earlier version of this manuscript.

REFERENCES

Anderson, O. L. 1961. Theoretical solutions for the secondary flow on the end wall of a vortex tube. *United Aircraft Corp., Rept. No. R-2494-I.*

Hama, F. R. 1941. The turbulent boundary layer along a flat plate. *Rept. Inst. Sci. Tech. (Tokyo) 1*, 13–19.

Lin, C. C. 1959. *Turbulent Flows and Heat Transfer*, p. 121. Princeton University Press, Princeton, N.J.

Ludwig, H. & Tillman, W. 1949. Investigation of the wall shearing stress in turbulent boundary layers. *NACA TM 1285.*

Rott, N. & Lewellen, W. S. 1964. Boundary layers in rotating flows. *Aerospace Corp., Rept. No. ATN-64 (9227)-6.*

Schlichting, H. 1968. *Boundary Layer Theory*, p. 564. McGraw-Hill, New York, N.Y.

Schultz-Grunow, F. 1941. New frictional resistance law for smooth plates. *NACA TM 986.*

Taylor, G. I. 1950. The boundary layer in the converging nozzle of a swirl atomizer. *Quart. J. Mech. Applied Math. 3*, part 2, 129–139.

von Karman, Th. 1921. Über laminare und tubulente Reibung, *ZAMM 1*, 233–247.

Weber, H. E. 1956. Boundary layer inside a conical surface due to swirl. *J. Applied Mech. 23*, 587–592.

Wieghart, K. 1944. On the turbulent friction layer for rising pressure. *NACA TM 1314.*

Ying, S. J. & Chang, C. C. 1968. Exploratory model study of tornado-like vortex dynamics. *The Catholic University of America, Rept. No. SSAP 68-002.*

ПРИЗЕМНЫЙ ТУРБУЛЕНТНЫЙ ПОГРАНИЧНЫЙ СЛОЙ В СТАЦИОНАРНОМ ТОРНАДООБРАЗНОМ ВИХРЕ

Недавно стали доступными экспериментальные данные по турбулентному пограничному слою у Земли в торнадо. Проделано сравнение с теориями Вебера, Андерсона, Ротта и Левелина и найдено, что средняя квадратичная ошибка велика и оправдывает появление улучшенной теории с новыми профилями скоростей, которые близки к экспериментальным данным. Показана в явном виде зависимость эволюции пограничного слоя от числа Рейнольдса. Настоящая теория распространяется на диапазон чисел Рейнольдса природного торнадо.